Redox Biology 14 (2018) 361–370

Contents lists available at ScienceDirect

Redox Biology

journal homepage: www.elsevier.com/locate/redox

Research Paper

The dual role of poly(ADP-ribose) polymerase-1 in modulating parthanatos and autophagy under oxidative stress in rat cochlear marginal cells of the stria vascularis

Hong-Yan Jiang[1], Yang Yang[1], Yuan-Yuan Zhang, Zhen Xie, Xue-Yan Zhao, Yu Sun, Wei-Jia Kong*

Department of Otorhinolaryngology, Union Hospital, Tongji Medical College, Huazhong University of Science and Technology, Wuhan 430022, China

ARTICLE INFO

Keywords:
Oxidative stress
PARP-1
Parthanatos
Autophagy
Marginal cells
Glucose oxidase

ABSTRACT

Oxidative stress is reported to regulate several apoptotic and necrotic cell death pathways in auditory tissues. Poly(ADP-ribose) polymerase-1 (PARP-1) can be activated under oxidative stress, which is the hallmark of parthanatos. Autophagy, which serves either a pro-survival or pro-death function, can also be stimulated by oxidative stress, but the role of autophagy and its relationship with parthanatos underlying this activation in the inner ear remains unknown. In this study, we established an oxidative stress model in vitro by glucose oxidase/glucose (GO/G), which could continuously generate low concentrations of H_2O_2 to mimic continuous exposure to H_2O_2 in physiological conditions, for investigation of oxidative stress-induced cell death mechanisms and the regulatory role of PARP-1 in this process. We observed that GO/G induced stria marginal cells (MCs) death via upregulation of PARP-1 expression, accumulation of polyADP-ribose (PAR) polymers, decline of mitochondrial membrane potential (MMP) and nuclear translocation of apoptosis-inducing factor (AIF), which all are biochemical features of parthanatos. PARP-1 knockdown rescued GO/G-induced MCs death, as well as abrogated downstream molecular events of PARP-1 activation. In addition, we demonstrated that GO/G stimulated autophagy and PARP-1 knockdown suppressed GO/G-induced autophagy in MCs. Interestingly, autophagy suppression by 3-Methyladenine (3-MA) accelerated GO/G-induced parthanatos, indicating a pro-survival function of autophagy in GO/G-induced MCs death. Taken together, these data suggested that PARP-1 played dual roles by modulating parthanatos and autophagy in oxidative stress-induced MCs death, which may be considered as a promising therapeutic target for ameliorating oxidative stress-related hearing disorders.

1. Introduction

Age-related hearing loss (ARHL) or presbycusis is the most prevalent sensory disorder among elderly individuals. ARHL is characterized by a progressive, bilateral, inevitable decline of hearing sensitivity with age and impaired ability of speech discrimination, detection and localization of sound [1]. Three classic types of presbycusis have been defined according to the pathological syndrome: sensory, neural and metabolic/strial [2]. However, the mechanism involved in presbycusis remains ambiguous. A prevalent proposed mechanism of presbycus is oxidative stress [3]. In this theory, an imbalance between reactive oxygen species (ROS) production and antioxidant ability, plays fundamental roles in aging and age-related diseases, including presbycusis [4]. ROS accumulation can oxidative major macromolecules such as lipids, proteins, and DNA leading to cellular damage [5].

The degenerative changes of stria vascularis and consequent reduction of endocochlear potential (EP) are regarded as the hallmarks of strial presbycusis [2,6]. The stria vascularis, located at the lateral wall of the cochlea, which is critical for the maintenance of the EP at steady state, is consisted of several subtype of cells, including the stria marginal cell (MC), the intermediate cell and the basal cell [7]. The MC is identified as a primary cell type for exploring the etiology of strial presbycusis based on its unique characters. On one hand, MCs express an array of ion channels, pumps and Na, K-ATPase, which correlates with overall strial function and normal EP [8]. On the other hand, due to its location and plentiful mitochondria, stria MC is particularly vulnerable to oxidative attacks, which will lead to the decline of EP, disturbance of the cochlear function and subsequently elevation of hearing thresholds [8].

Poly(ADP-ribose) polymerase-1 (PARP-1) is an abundant nuclear

* Corresponding author.
E-mail address: entwjkong@hust.edu.cn (W.-J. Kong).
[1] These authors contributed equally to this work.

http://dx.doi.org/10.1016/j.redox.2017.10.002
Received 1 August 2017; Received in revised form 1 October 2017; Accepted 3 October 2017
Available online 07 October 2017

enzyme playing a prominent role in DNA damage repair, genomic integrity maintenance and execution of cell differentiation and death [9]. Various agents including ROS, ultraviolet (UV) light, alkylating agents inflicted DNA damage can activate PARP-1 [10,11]. Once PARP-1 is overactivated, it will results in rapid depletion of NAD + and ATP accompanied with excessive polyADP-ribose (PAR) polymer synthesis, ultimately leading to irreversible energy failure and detrimental effects, which have been implicated in different tissue types such as brain, liver, heart, lung, retina, kidney and skeletal muscle [12,13]. It has been well demonstrated that inhibiting PARP-1 overactivation improves the therapeutic efficacy in multiple disease models characterized by DNA damage, including ischemia, diabetes, shock, inflammation and cancer [14]. Besides, accumulated PAR polymers via PARP-1 activation can induce cell death through a mechanism defined as PARP-1-dependent cell death (parthanatos) by translocating from nucleus to mitochondria, where it binds to apoptosis-inducing factor (AIF) and triggers AIF translocation to the nucleus [15,16]. Parthanatos, a specific modality of cell death distinct from other types of cell death such as caspase-dependent apopotosis and necrosis is characterized by biochemical features including hyper-activation of PARP-1, excessive PAR polymer synthesis, mitochondrial depolarization and nuclear translocation of AIF [17]. Nuclear condensation and cellular propidium iodide (PI) positive staining after the initiation of parthanatos are its morphological features [18]. Pharmacological inhibition or genetic deletion of PARP-1 and AIF have been shown to abrogate parthanatos and ameliorate cell injury induced by oxidative stress in a variety of cell types like fibroblasts, neurons, and HeLa cells [18,19]. It has been reported that oxidative stress is able to induce autophagy, and autophagy contributes to sequestering oxidative biomolecules and organelles in turn [20]. Autophagy is a conserved self-degradation process in which aged, dysfunctional and/or damaged organelles and material are delivered to lysosomes for breakdown and then recycled by the cells [21]. It plays a crucial role for maintaining cellular homeostasis and health via removal of disposable or potentially harmful constituents, and the beneficial functions of autophagy have been observed in numerous cell types such as neurons, hepatocytes, T lymphocyte [22]. Although autophagy is generally considered as a cytoprotective mechanism against various stress stimuli, autophagy can mediate autophagic cell death in some rare cases [23]. Autophagy dysfunction is associated with several diseases such as neurodegeneration, infection, cancer, and heart diseases [24]. PARP-1 activation induced by DNA damage has been suggested to be involved in amplifying cytoprotective autophagy [25], and inhibition of PARP-1 causes the delay or suppression of pro-survival autophagy [26–28].

During normal aerobic metabolism, low concentrations of ROS are continuously generated in living organisms [29]. Among the different species of ROS, hydrogen peroxide (H_2O_2) is generated by nearly all sources of oxidative stress, and can cross cell membranes freely [30,31]. Though the rate of H_2O_2 generation varies for different types of cell, the production in vivo is continuous, with a steady-state level fluctuating within the range of 10^{-8} to 10^{-7} M [32]. In the majority of previous studies, H_2O_2 was added directly to the cells as a bolus, so cells were initially exposed to relatively high concentrations of H_2O_2 followed by a rapid reduction, because of the constant H_2O_2 consumption [33]. In contrast, glucose oxidase (GO), which could continuously generate low concentrations of H_2O_2 by catalyzing its substrate of glucose (G), was used to mimic continuous exposure to H_2O_2 in physiological conditions, and represented a superior method of H_2O_2 delivery.

Considering the association of PARP-1 with both autophagy and parthanatos, it is justified to speculate that they are interconnected via PARP-1 or downstream molecules of PARP-1 activation. Since the relationship between parthanatos and autophagy, and the functional role of autophagy in MCs remain unreported, in this study, we used GO/G to mimic the states of oxidative stress in vivo. We found that GO/G stimulated parthanatos and autophagy in MCs via PARP-1 activation. We also investigated the correlation between GO/G-induced parthanatos and autophagy, and found that autophagy inhibition by 3-Methyladenine (3-MA) exacerbated parthanatos, demonstrating a pro-survival role for autophagy in response to GO/G in MCs.

2. Materials and methods

2.1. Isolation, culture and identification of primary MCs

All experimental procedures in this study were in accordance with the National Institutes of Health Guide for the Care and Use of Laboratory Animals and approved by Ethics Committee of Huazhong University of Science and Technology. Isolation and culture of primary MCs have been described in our previous report [34]. Briefly, stria vascularis tissue, which was isolated from neonatal (3 days old) Sprague Dawley (SD) rats, was dissected, minced and then followed by digestion with 0.1% collagenase II (Sigma-Aldrich, St. Louis, MO, USA) for 30 min at 37 °C. Then the samples were centrifuged for 5 min at 800 g and plated in Epithelial Cell Medium-animal (EpiCM-animal, ScienCell, USA) at 37 °C in a humidified incubator with 5% CO2. The identification of primary MCs by cytokeratin-18, a characteristic molecule of MCs [35,36], was performed as described previously [37].

2.2. Cell viability assay

After the MCs fused into a monolayer, cells were resuspended and plated in 96-well culture plates at 1×10^4 cells per well in quintuple for the CCK-8 colorimetric assay (Dojindo, Tokyo, Japan). In brief, after incubating for 48 h, the MCs were treated for 4 h with different concentrations of GO (0 U/L, 10 U/L, 20 U/L, 30 U/L, 40 U/L, 50 U/L, 60 U/L, 70 U/L, 80 U/L, 100 U/L) (Sigma-Aldrich) in the fresh EpiCM-animal medium supplemented with 5 mM G (Sigma-Aldrich). Then the medium was replaced with 100 μl fresh complete growth medium and 10 μl of CCK-8 solution. After incubation for 2 h at 37 °C in the dark, the absorbance of per well was recorded at 450 nm using a microplate reader (Bio-Tek, Colmar, France).

2.3. Measurement of ROS production

2′,7′-dichlorofluorescin diacetate (DCFH-DA, Sigma-Aldrich) which can be oxidized into highly fluorescent dichlorofluorescein (DCF) in the presence of ROS, was used to determine the intracellular ROS level. Briefly, after exposed to GO/G for indicated incubation time, the treated cells were harvested and incubated with DCFH-DA (20 μM) for 20 min in the dark at 37 °C. Then, the MCs were washed three times with DMEM/F12 (Hyclone, Logan, UT, USA). The fluorescence signals were recorded using flow cytometry (Olympus, Tokyo, Japan), and mean fluorescence intensity was calculated with GraphPad Prism 5.0 software.

2.4. Cell treatment and transfection

The MCs were incubated with 60 U/L GO for 4 h in the fresh EpiCM-animal medium supplemented with 5 mM G to induce oxidative stress. The GO/G (0 U/L GO/5 mM G) group was considered as a control. For achieving autophagy inhibition, 3-MA (10 mM, 1 h) (Sigma-Aldrich) was applied to MCs prior to GO/G treatment.

The recombinant adenoviruses for interference vector of PARP-1 (Ad-PARP-1-RNAi) and control vector (Ad-Con) were purchased from GeneChem (Shanghai, China). MCs transfection was performed as described previously [37]. A multiplicity of infection (MOI; 30) for Ad-Con and Ad-PARP-1-RNAi was used. Briefly, MCs were cultured in EpiCM-animal medium containing Ad-PARP-1-RNAi or Ad-Con for 4 h. Then the medium was replaced with fresh EpiCM-animal medium and transfected MCs were incubated for 48 h before subsequent experiments.

2.5. Immunofluorescence staining

MCs were seeded in confocal dishes and treated as designated. After corresponding treatment, the cells were fixed in 4% paraformaldehyde for 15 min at room temperature, washed three times with phosphate buffered saline (PBS, pH 7.4) and then permeabilized with 0.3% Triton X-100 for 20 min. After blocking with 5% bovine serum albumin (BSA) for 10 min, the cells were incubated with primary antibody against PAR (1:100, Enzo Life Sciences, Farmingdale, NY, USA), AIF (1:50, Abcam, Cambridge, UK, USA), LC3 (1:100, Sigma-Aldrich) overnight at 4 °C. Then the cells were washed with PBS and incubated with flurochrome-conjugated secondary antibody against mouse (1:100, Abbkine, Redlands, CA, USA) or rabbit (1:100, AntGene, Wuhan, China) for 1 h at room temperature. The specimens were counterstained with DAPI (Beyotime Biotec, Jiangsu, China) for nuclei for 5 min, and then observed by laser-scanning confocal microscope (Nikon, Japan).

2.6. Mitochondrial membrane potential (MMP) measurement

The MMP changes were measured by Mitochondrial membrane potential assay kit with JC-1 (Beyotime) according to the manufacturer's instructions. Briefly, treated cells were harvested and washed with cold PBS twice. Thereafter, the cells were resuspended in mixture of 500 μl culture medium and 500 μl JC-1 staining fluid for 20 min protected from light at 37 °C. Subsequently, cells were washed with cold staining buffer for three times prior to flow cytometry (Olympus, Tokyo, Japan). JC-1 exists either as cytoplasmic JC-1 monomer or mitochondrial J-aggregates depending on the potential of the mitochondrial membrane. In healthy cells with high MMP, JC-1 spontaneously forms J-aggregates in mitochondria which emits red fluorescence. However, in unhealthy cells, the MMP declines and JC-1 is released from mitochondria and exists as monomer in the cytoplasm, which yields green fluorescence. Thus, MMP can be indicated by the ratio of red to green fluorescence intensity. Carbonyl cyanide 3-chlorophenylhydrazone (CCCP), which disrupted mitochondrial integrity and induced the complete loss of MMP, was used as a positive control.

MMP changes in MCs were also detected in situ using the JC-1 assay. After corresponding treatment, the cells were stained with JC-1 as described above and visualized by laser-scanning confocal microscope (Nikon, Japan).

2.7. Annexin V/PI staining

Cell death modality was determined by Annexin V-FITC Apoptosis Detection Kit (KeyGen Biotech, China). Briefly, after treatment as designated, MCs were harvested via trypsinization, rinsed twice with cold PBS and resuspended in 500 μl of binding buffer. Then the specimens were stained with 5 μl of Annexin V-FITC and 5 μl of PI for 15 min in the dark at room temperature. The stained MCs were analyzed by flow cytometry (Olympus, Tokyo, Japan).

2.8. Western blot analysis

Total proteins were extracted with RIPA lysis buffer (Beyotime) containing 1% proteinase inhibitors (Beyotime). The mitochondria isolation followed the instructions of the Cell Mitochondria Isolation Kit (Beyotime). Nuclear and cytoplasmic proteins were isolated using a Nuclear and Cytoplasmic Protein Extraction Kit (Beyotime). The protein concentrations were quantified using a BCA Protein Assay Kit (Beyotime). Equal amounts of protein samples were subjected to 10–12% SDS-PAGE separation and then transferred to the polyvinylidene difluoride membrane (Millipore, Boston, MA, USA). Subsequent procedures were performed as described previously [38]. The following antibodies were used: rabbit anti-PARP-1 (1: 500, Santa Cruz, CA, USA), rabbit anti-AIF (1:1000, Abcam), rabbit anti-LC-3 (1:1000, Sigma-Aldrich), rabbit anti-p62 (1:1000, Cell Signaling Technology, MA, USA), mouse anti-PAR (1:1000, Enzo Life Sciences), mouse anti-β-actin (1:5000, Abbkine), rabbit anti-COX IV (1:1000, Proteintech, Wuhan, China), mouse anti-Histone H3 (1:3000, Abbkine), HRP-conjugated secondary antibodies (1:5000, Abbkine). Protein bands were detected by enhanced chemiluminescence kit (Thermo, USA).

2.9. Statistical analyses

All experiments were performed independently at least in triplicate. Statistical analysis was conducted by using GraphPad Prism 5.0. The values are the mean ± S.E.M. Statistical comparisons were analyzed using Student's unpaired *t*-test or unpaired *t*-test with Welch's correction to assess the significance of difference between results. Values of P less than 0.05 were considered to indicate statistical significance.

3. Results

3.1. The viability and intracellular ROS level of MCs following GO/G stimulation

GO/G cytotoxicity was evaluated by CCK-8 assay. A concentration-dependent decrease of MCs viability was observed at > 20 U/L GO. However, GO concentrations between 20 and 50 U/L only induced a detectable, but not statistically significant reduction of MCs viability, compared with the control group (Fig. 1A). At a concentration of GO/G (60 U/L GO/5 mM G), GO/G significantly decreased MCs viability in comparison with the control ($P < 0.01$). Next, flow cytometry were performed to evaluate the intracellular ROS level following exposure to GO/G (60 U/L GO/5 mM G) for different times, and revealed a significant time-dependent increase of intracellular ROS level (Fig. 1B). After exposure of MCs to GO/G (60 U/L GO/5 mM G) for 4 h, ROS intensity was 2.86-fold of the control group (Fig. 1B). These data showed that GO/G (60 U/L GO/5 mM G) stimulation remarkably reduced MCs viability and increased intracellular ROS level in MCs. Therefore, GO/G (60 U/L GO/5 mM G) was used in subsequent experiments.

3.2. GO/G induced parthanatos in MCs

Intracellular ROS production has been demonstrated to be involved in the regulation of parthanatos [39]. To investigate whether GO/G initiated parthanatos in MCs, we measured the formation of PAR polymer by immunoflurescence and western blot. Western blot results showed that the expression of PAR polymer obviously increased in a time-dependent manner after GO/G treatment (Fig. 2A). Immunofluorescence results also confirmed the increased cytoplasmic expression of PAR polymer in GO/G (60 U/L GO/5 mM G, 4 h) treated cells compared with control (Fig. 2B). Meanwhile, GO/G treatment could lead to the elevation of PARP-1 protein levels in mitochondria, cytoplasm and nuclear compared with controls (Fig. 2C). These results suggested that GO/G induced the activation and accumulation of PARP-1 in MCs.

Mitochondria, commonly known as the powerhouse of the cell, play fundamental roles in maintaining basic cellular functions. Mitochondria dysfunction under stress conditions facilitates the release of apoptosis-related substances from the mitochondria such as AIF [40]. In addition, abnormal accumulation of PAR polymer causes cell death via inducing mitochondrial depolarization [39]. We monitored the changes of MMP using JC-1 staining by flow cytometry and in situ staining after GO/G treatment. Flow cytometry data revealed that MMP significantly declined in a time-dependent manner in GO/G treated MCs (Fig. 3A). In consistent with the flow cytometry results, a time-dependent decrease of the red fluorescence and elevation of the green fluorescence were observed by confocal microscopy in GO/G treated group (Fig. 3B). These data demonstrated that GO/G could provoke mitochondrial depolarization in MCs.

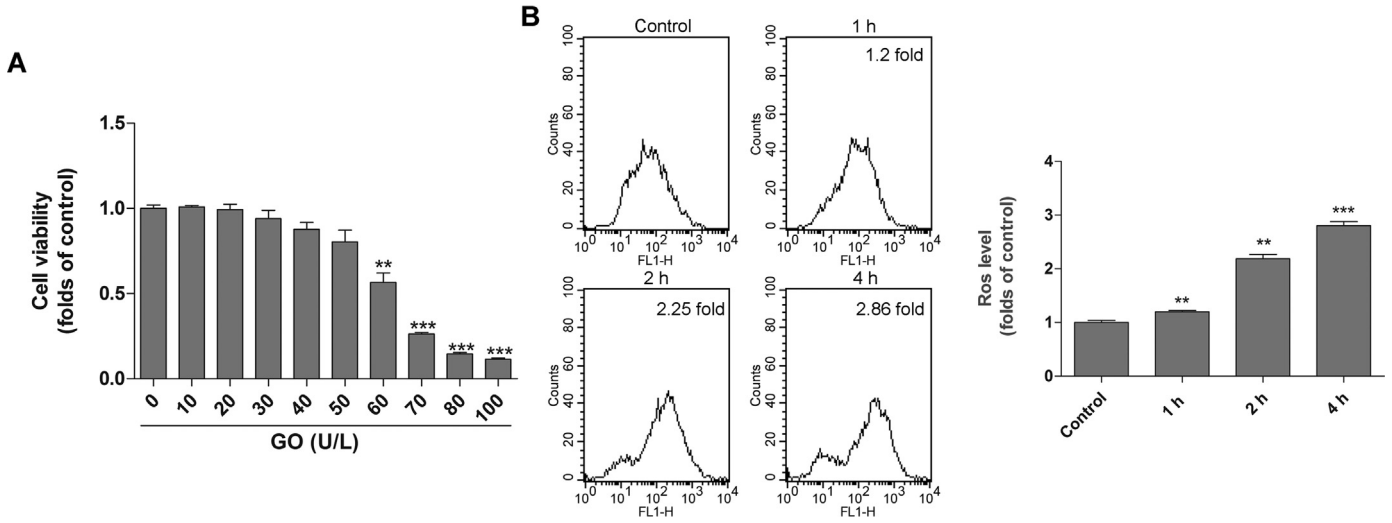

Fig. 1. GO/G inhibited MCs viability and increased intracellular ROS production. (A) MCs were treated with GO/G (0–100 U/L GO/5 mM G) for 4 h. Cell viability was assessed by CCK-8 assay. The GO/G (0 U/L GO/5 mM G) group was considered as the control. The MCs' viability was strongly suppressed by higher concentrations than GO/G (60 U/L GO/5 mM G). (B) MCs were treated with GO/G (60 U/L GO/5 mM G) for different times and then stained with DCFH-DA for flow cytometry analysis. Statistical analysis showed the up-regulation of intracellular ROS production in a time-dependent manner following GO/G (60 U/L GO/5 mM G) treatment in MCs. Data are expressed as mean ± S.E.M. Representative results of at least three experiments are shown (** $P < 0.01$ and *** $P < 0.0001$).

Previous studies have reported that the accumulation of PAR polymer due to PARP-1 activation could promote the release of AIF from the mitochondria, which played a pivotal role in parthanatos [16]. Based on the above observations, we detected mitochondria, cytoplasm and nuclear AIF levels by performing immunoflurescence and Western blot. After GO/G treatment, AIF protein distribution in the mitochondrial fraction was significantly decreased, with predominant increase in the cytoplasmic and nuclear fraction, compared with the control (Fig. 2C). Consistently, confocal microscopy results revealed an obvious accumulation of AIF within the nucleus after GO/G stimulation

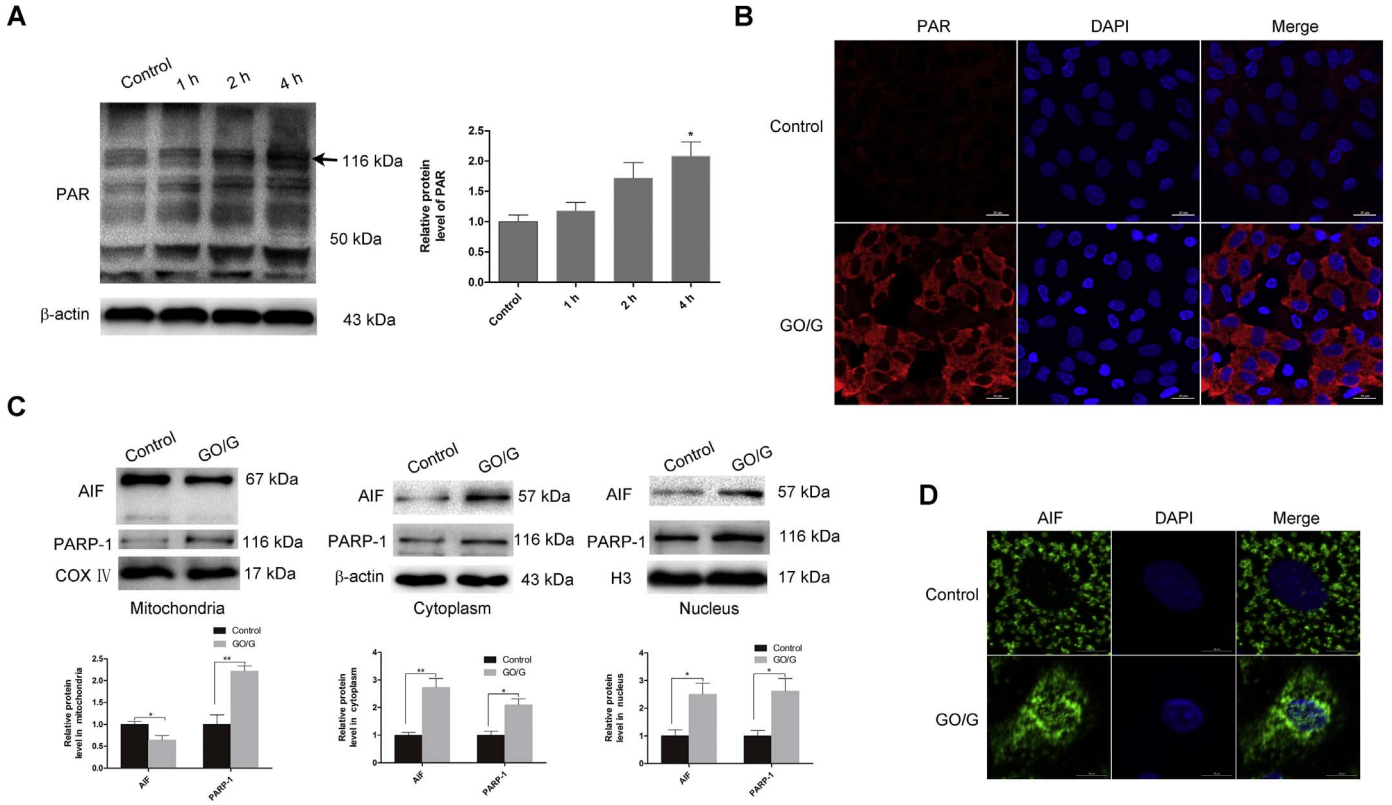

Fig. 2. GO/G up-regulated the expression of parthanatos-related proteins. (A) Western blot analysis of PAR polymer levels in MCs following treatment with GO/G (60 U/L GO/5 mM G) for various times. β-actin was used as a loading control. (B) Immunofluorescent analysis of the accumulation of PAR polymer (red) in MCs upon treatment with GO/G (60 U/L GO/5 mM G) for 4 h by confocal microscopy. Nuclei were stained with DAPI (blue). Scale bars: 20 μm. (C) After GO/G (60 U/L GO/5 mM G) treatment for 4 h, mitochondrial, cytoplasmic and nuclear fractions were isolated from the treated cells and subjected to western blot for detection of the protein levels of PARP-1 and AIF. COX IV was used as a mitochondrial fraction loading control. β-actin and H3 were used as cytoplasmic and nuclear loading control respectively. (D) MCs were treated as above to detect the translocation of AIF from mitochondria to nucleus by confocal microscopy. AIF was shown in green and nuclei were stained with DAPI (blue). Scale bars: 10 μm. Data are expressed as mean ± S.E.M. Representative results of three experiments are shown (* $P < 0.05$ and ** $P < 0.01$).

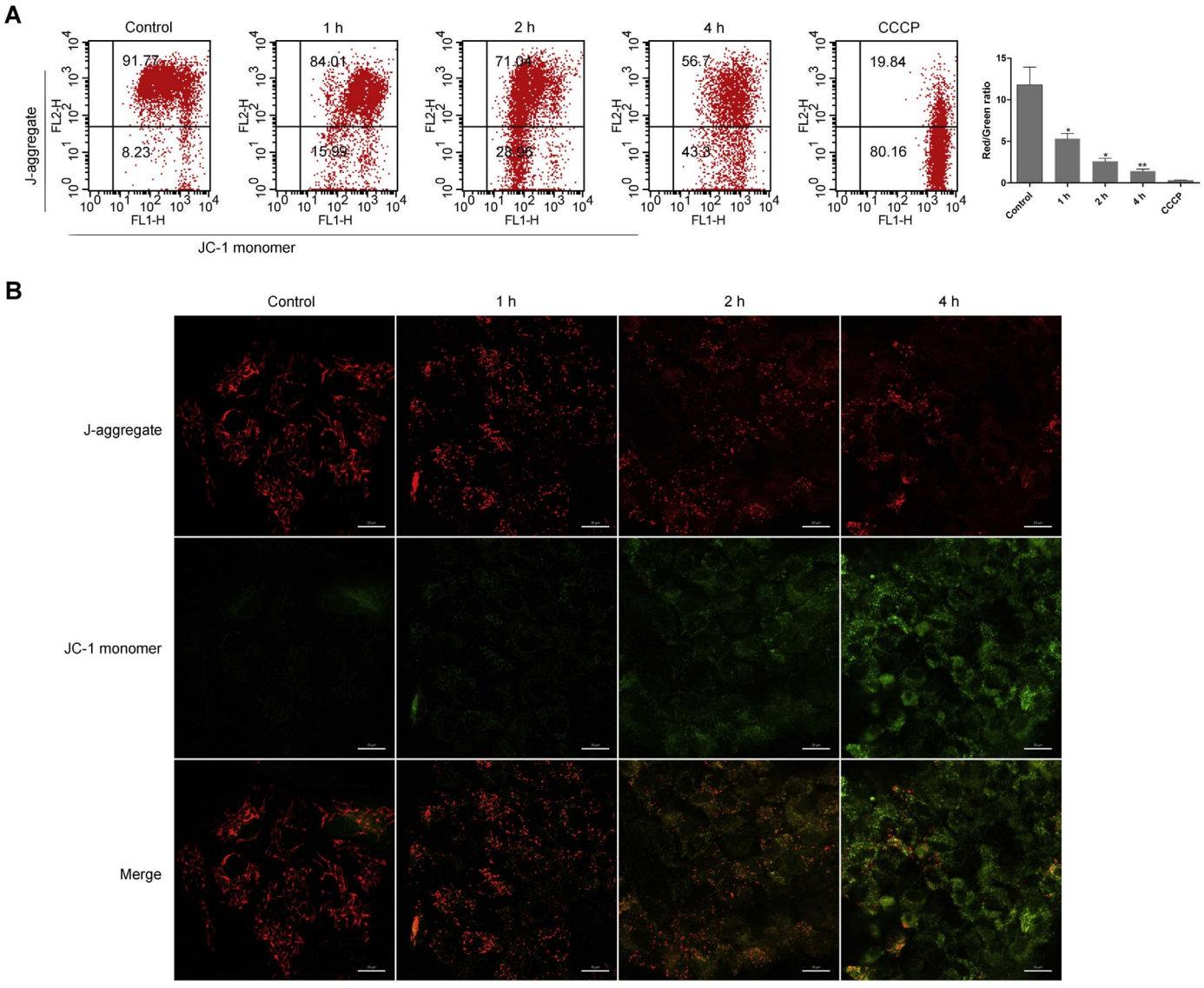

Fig. 3. GO/G induced mitochondrial depolarization. (A) The cells were treated with GO/G (60 U/L GO/5 mM G) for various times, stained with JC-1 and analyzed by flow cytometry with quantification showing decreased ratios of red/green fluorescence intensity after GO/G (60 U/L GO/5 mM G) treatment. CCCP was used as a positive control. JC-1 monomer: green; J-aggregate: red. (B) MCs treated as above were labeled with fluorescent probe JC-1 to evaluate MMP changes in situ by confocal microscopy. Representative micrographs showed that the control cells displayed higher level of red fluorescence, whereas GO/G-treated cells exhibited higher level of green fluorescence. J-aggregate: red; JC-1 monomer: green. Scale bars: 20 μm. Data are expressed as mean ± S.E.M. Representative results of at least three experiments are shown (* $P < 0.05$ and ** $P < 0.01$).

(Fig. 2D). Altogether, these results indicated that GO/G triggered parthanatos via upregulation of PARP-1 protein levels, accumulation of PAR-polymer, mitochondrial depolarization and translocation of AIF into nucleus which represented all the signatures of parthanatos in MCs.

3.3. Downregulation of PARP-1 ameliorated GO/G-induced parthanatos in MCs

To investigate the role of PARP-1 in GO/G-induced parthanatos, loss of function study via PARP-1 knockdown was performed. Western blot showed that the protein expression of PARP-1 was remarkably reduced after PARP-1 knockdown (Fig. 4D). To confirm whether the accumulation of PAR polymer was mediated by PARP-1, we examined the effects of PARP-1 knockdown on PAR polymer accumulation by western blot. As shown in Fig. 4C, PARP-1 knockdown dramatically reduced GO/G-induced PAR polymer accumulation. Then we performed Annexin V-FITC and PI staining to evaluate the effect of PARP-1 knockdown on GO/G-induced MCs death. As shown in Fig. 4A, PARP-1 knockdown protected MCs against GO/G-induced parthanatos as evidenced by the reduced proportion of PI positive cells (PI+). To assess the effect of PARP-1 knockdown on GO/G-induced mitochondrial depolarization, JC-1 staining was performed and it proved that PARP-1 knockdown could partially reverse GO/G-induced MMP decline (Fig. 4B). Accumulating evidence confirmed that the AIF nuclear translocation was associated with the activation of PARP-1 [17,41]. Thus, we examined the protein levels of AIF in the PARP-1 knockdown samples, and found that knockdown of PARP-1 remarkably reduced the release of AIF from mitochondria to the cytoplasm and nucleus after GO/G treatment (Fig. 4D). Confocal microscopy results also indicated that PARP-1 knockdown reduced GO/G-induced accumulation of AIF within the nucleus (Fig. 4E). Taken together, these results suggested that GO/G-induced parthanatos in MCs was PARP-1-dependent.

3.4. PARP-1 knockdown suppressed GO/G-induced autophagy in MCs

ROS has been implicated in stimulating autophagy [20]. To identify autophagy induction by GO/G in MCs, we evaluated the level of autophagy in MCs after GO/G treatment by detecting the protein levels of

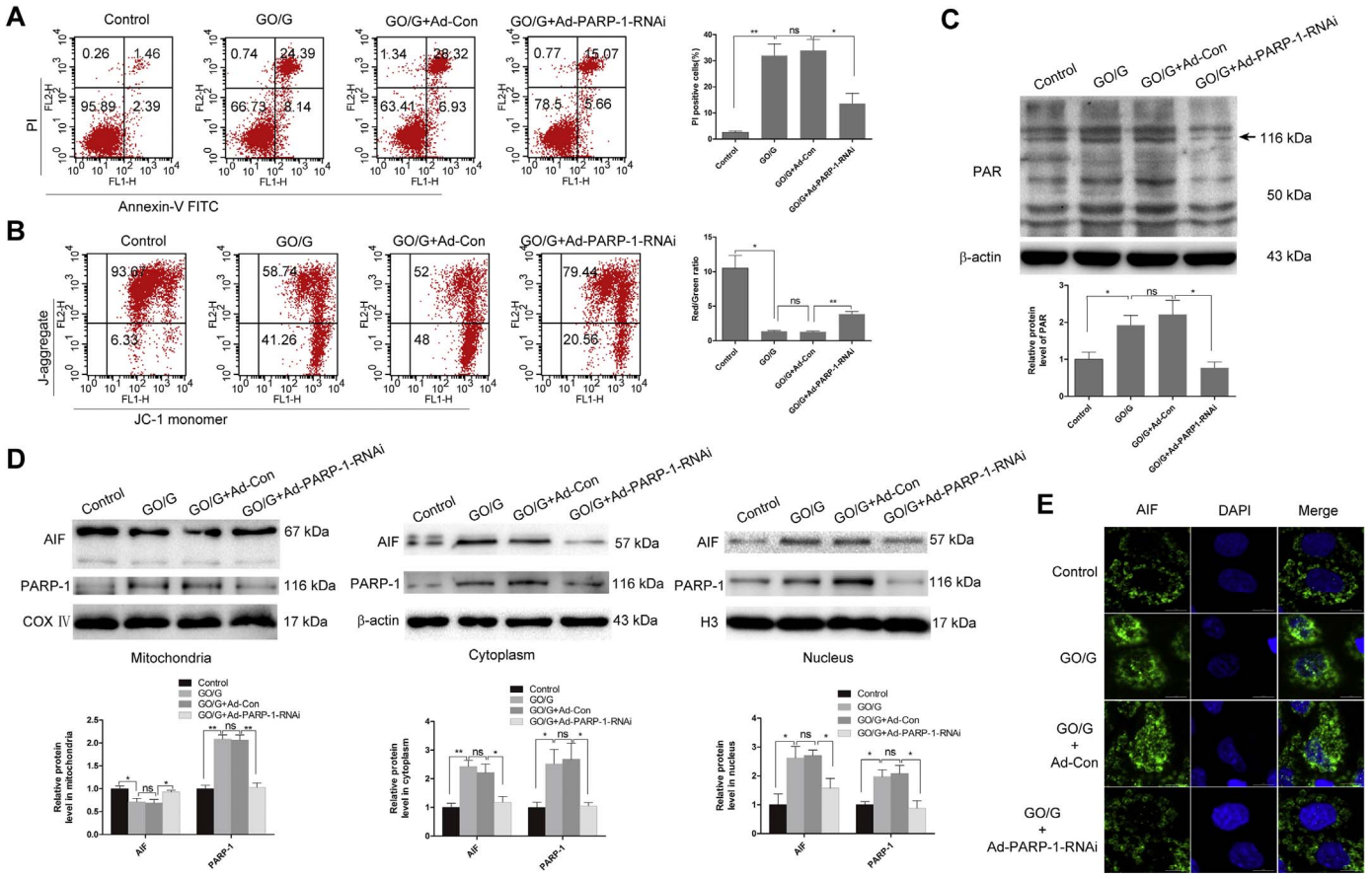

Fig. 4. PARP-1 knockdown ameliorated GO/G-induced parthanatos. MCs were transfected with Ad-PARP1-RNAi or Ad-control-RNAi (Ad-Con) recombinant virus. 48 h after transfection, MCs were treated with GO/G (60 U/L GO/5 mM G) for 4 h. (A) Annexin V/PI staining and flow cytometry analysis of cell death. Percentages of PI positive cells are shown. (B) JC-1 staining and flow cytometry analysis of MMP. The ratios of red/green fluorescence intensity are shown. JC-1 monomer: green; J-aggregate: red. (C) The accumulation of PAR polymer was measured by western blot. The level of β-actin was used as a loading control. (D) The mitochondrial, cytoplasmic and nuclear levels of PARP-1 and AIF were analyzed by western blot. COX IV was used as a mitochondrial fraction loading control. β-actin and H3 were used as cytoplasmic and nuclear loading control respectively. (E) The detection of translocation of AIF from mitochondria to nucleus by confocal microscopy. AIF is shown in green and nuclei were stained with DAPI (blue). Scale bars: 10 μm. Data are expressed as mean ± S.E.M. Representative results of three experiments are shown (* $P < 0.05$ and ** $P < 0.01$).

LC3-II and p62. Western blot showed that the LC3-I to LC3-II conversion significantly increased, while the protein levels of p62 dramatically reduced in a time-dependent manner after GO/G treatment (Fig. 5A). Compared with the GO/G treated alone group, preincubation with autophagy inhibitor 3-MA for 1 h to block autophagosome formation before exposure to GO/G induced a significant reduction of LC3-II protein and a notable increase of p62 (Fig. 5B). In addition, the immunofluorescence detection of LC3 showed that punctate fluorescence was visible following GO/G treatment in MCs, and the signal significantly decreased in presence of autophagy inhibitor (Fig. 5C). To confirm whether PARP-1 is involved in regulating autophagy in MCs, we evaluate the expression of LC3-II and p62 by western blot in PARP-1 knocked down cells. The data showed that PARP-1 knockdown greatly attenuated GO/G-induced conversion of LC3-I to LC3-II, and remarkably reversed the decline of p62 protein levels in comparison with the control (Fig. 5D). These findings indicated that PARP-1 activation contributed to the regulation of GO/G-induced autophagy in MCs.

3.5. Autophagy served as a protective mechanism against GO/G-induced parthanatos in MCs

To elucidate the functional role of autophagy in MCs, and the possible relationship between GO/G-induced parthanatos and autophagy, autophagy inhibitor 3-MA was used and the effect on GO/G-induced cell death was evaluated by performing Annexin V and PI staining. As shown in Fig. 6A, pretreatment with 3-MA accelerated GO/G-induced parthanatos as evidenced by the increased percentage of PI positive cells compared with GO/G treatment alone. Moreover, we observed that 3-MA pretreatment aggravated GO/G-induced MMP decline (Fig. 6B). As a further confirmation, we analyzed the expression of parthanatos-related proteins with or without 3-MA treatment. As shown in Fig. 6C, 3-MA pretreatment led to a noticeable increase of PAR polymer synthesis. The elevation of PARP-1 levels in mitochondria, cytoplasm and nuclear were observed, indicating that PARP-1 activation was further boosted by the inhibition of autophagy (Fig. 6D). Furthermore, pretreatment of 3-MA facilitated GO/G-induced decline of mitochondria AIF levels and elevation of cytoplasm and nuclear AIF levels, demonstrating that autophagy inhibition sensitized MCs to GO/G-induced cell death (Fig. 6D). These results indicated that autophagy played a pro-survival role against GO/G-induced parthanatos in this context.

4. Discussion

Present study aimed to explore the modes of cell death involved in oxidative stress-induced MCs death, with a special emphasis on the regulatory role of PARP-1 in this process for developing effective treatment strategies against hearing disorders in strial presbycusis. Here we demonstrated that GO/G induced parthanatos and autophagy in MCs, and both of them were closely associated with the activation of PARP-1. PARP-1 knockdown ameliorated GO/G-induced parthanatos and diminished GO/G-induced autophagy. Additionally, we revealed

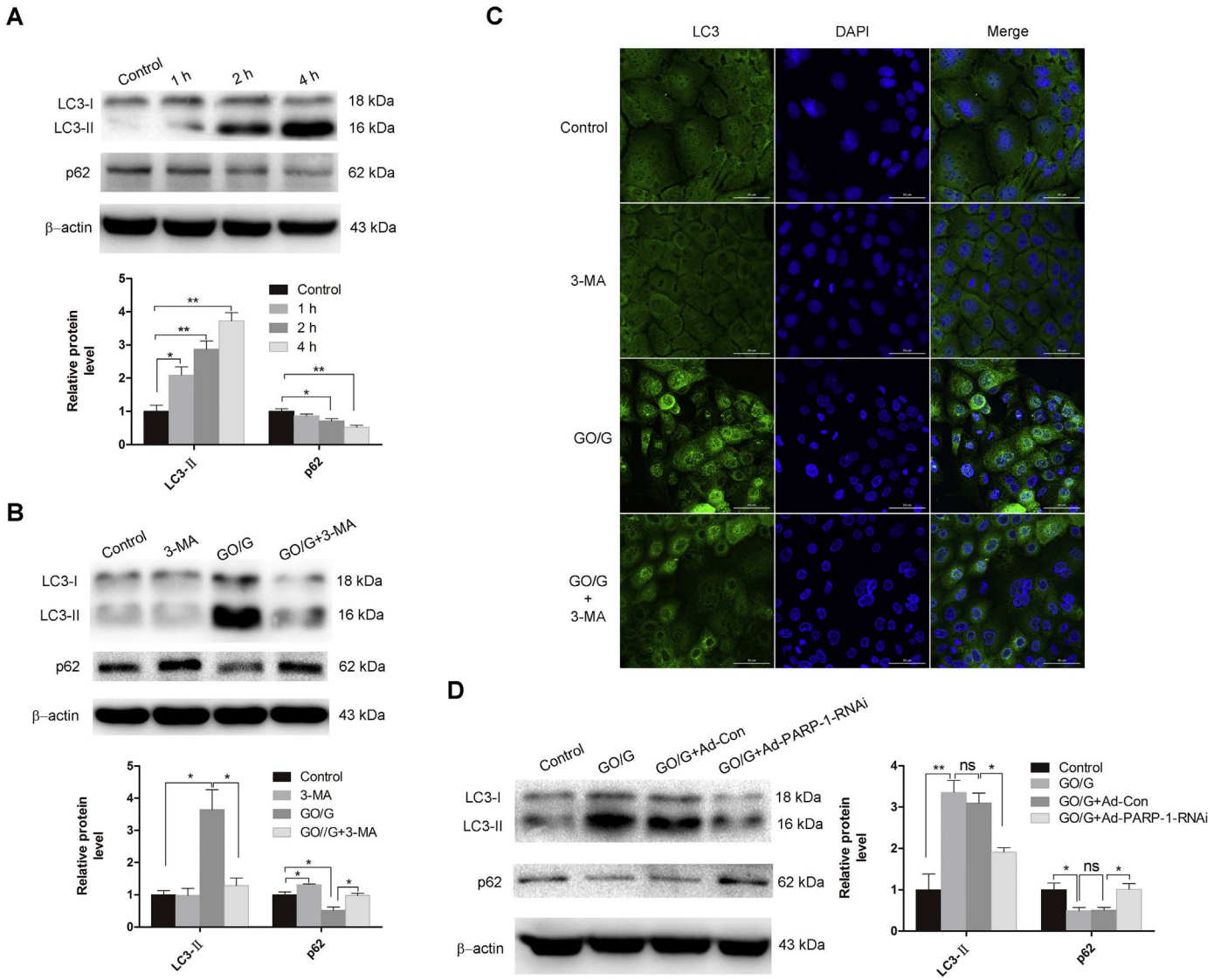

Fig. 5. PARP-1 knockdown suppressed GO/G-induced autophagy. (A) Autophagy measurement by detection of the expression of p62 protein and the conversion of LC3-I to LC3-II by western blot. The MCs were treated with GO/G (60 U/L GO/5 mM G) for various times. The level of β-actin was used as a loading control. (B) Measurement of p62 protein levels and the conversion of LC3-I to LC3-II following GO/G (60 U/L GO/5 mM G) treatment with or without 3-MA pretreatment (5 mM) by western blot. β-actin was used as a loading control. (C) Detection of autophagosomes using immunostaining with LC3 antibody by confocal microscope. Cells were treated with GO/G (60 U/L GO/5 mM G) for 4 h with or without 3-MA pretreatment (5 mM). LC3 is shown in green and nuclei were stained with DAPI (blue). Scale bars: 50 μm. (D) Western blot analysis of protein levels of p62 and the conversion of LC3-I to LC3-II following GO/G treatment with or without PARP-1 knockdown. β-actin was used as a loading control. Data are expressed as mean ± S.E.M. Representative results of three experiments are shown (* $P < 0.05$ and ** $P < 0.01$).

that inhibition of autophagy by 3-MA accelerated GO/G-induced parthanatos, proving a pro-survival role of autophagy in response to GO/G in MCs. Altogether, our results suggested that PARP-1 played dual roles in response to oxidative stress in MCs.

PARP-1 activation in response to mild DNA damage is responsible for cellular DNA damage repair and maintenance of cellular homeostasis whereas PARP-1 over-activation due to massive DNA damage causes excessive synthesis of PAR polymer, which plays pivotal roles in the induction of AIF mediated parthanatos [17]. Distinct from apoptosis, parthanatos process is not accompanied with the formation of apoptotic body. While these two modes of cell death share some similar characteristics such as externalization of phosphatidylserine, dissipation of MMP, and chromatin condensation [17]. Previous studies have reported the induction of parthanatos in multiple pathological conditions including diabetes, inflammation, cerebral hypoxia/ischemia and trauma, as well as in various tumor cell death induced by chemical [42–47]. Chiu et al. [48]. reported that oxidative stress induced by an alkylating agent of MNNG initiated parthanatos in the mouse embryonic fibroblasts. To identify the involvement of parthanatos in oxidative damage of MCs, we first established an in vitro cellular oxidative stress model by GO/G, which could generate H_2O_2 in a low and continuous manner mimicking the physiological condition, since tissues and cells in vivo are exposed to continuously generated H_2O_2 in most cases. Our data showed that GO/G (60 U/L GO/5 mM G) treatment significantly decreased the viability of MCs and remarkably increased the intracelluar ROS in a time-dependent manner. Consistent with our previous observations [37], GO/G treatment induced excessive PAR polymer accumulation in MCs. Although PAR polymer is originally synthesized in the nucleus, it will translocate to the cytoplasm thereafter. Immunofluorescence staining revealed that the elevated PAR polymer after 4 h GO/G treatment was mainly located in cytoplasm of MCs. Moreover, PARP-1 expressions in mitochondria, cytoplasm and nucleus were enhanced after GO/G treatment. These indicated the activation and upregulation of PARP-1 after GO/G treatment, which was an pivotal step of parthanatos induction.

Due to the susceptibility of mitochondria to oxidative damage, we

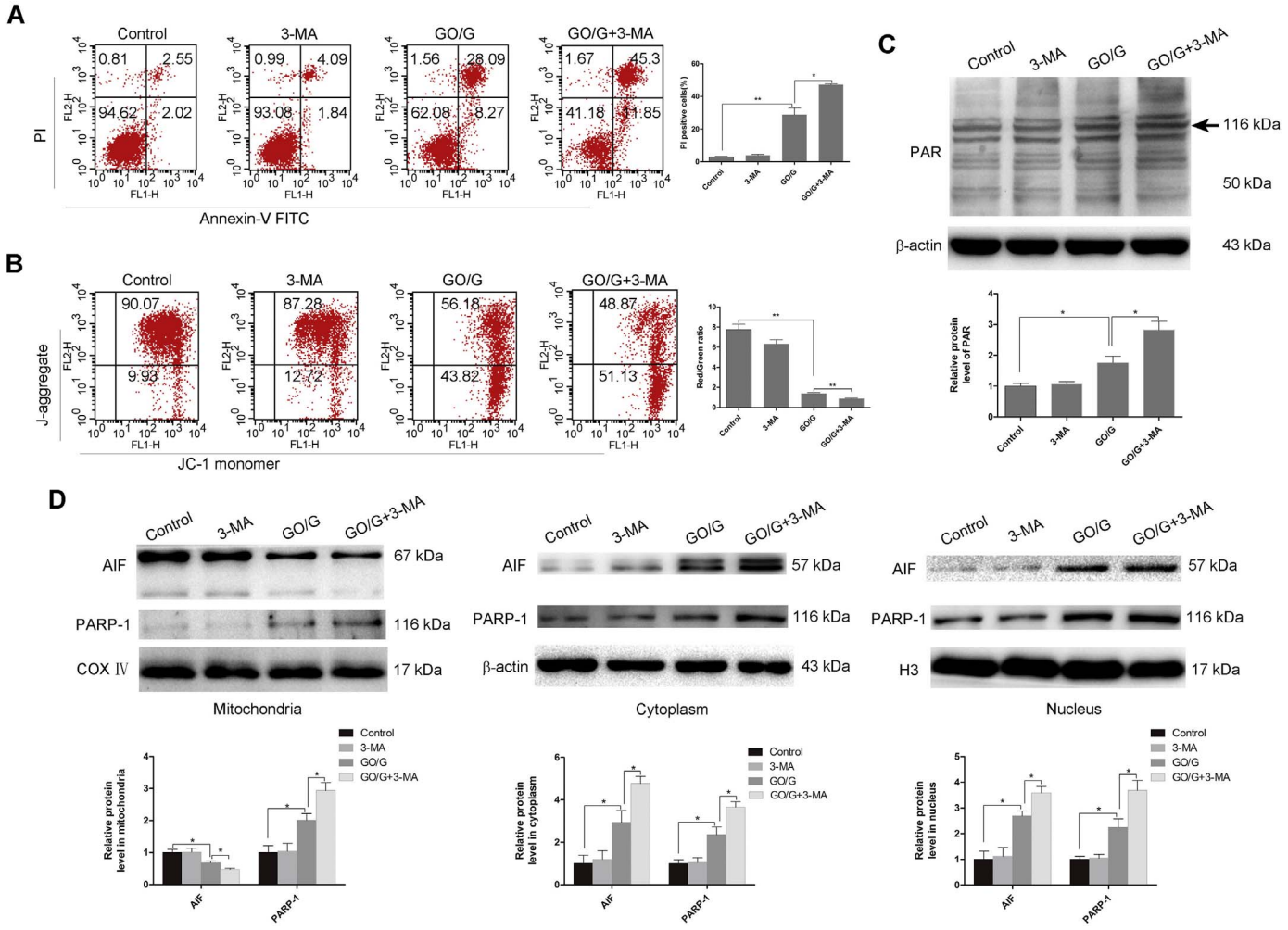

Fig. 6. Autophagy inhibition sensitized MCs to GO/G-induced parthanatos. (A) Annexin V/PI staining and flow cytometry analysis of cell death. MCs were treated with GO/G (60 U/L GO/5 mM G) for 4 h with or without 3-MA pretreatment (5 mM). Percentages of PI positive cells are shown. (B) JC-1 staining and flow cytometry analysis of MMP. Cells were treated as above. The ratios of red/green fluorescence intensity are shown. JC-1 monomer: green; J-aggregate: red. (C) The accumulation of PAR polymer was measured by western blot. Cells were treated as above and subjected to western blot analysis. β-actin was used as a loading control. (D) The protein levels of PARP-1 and AIF in the mitochondrial, cytoplasmic and nuclear fractions of MCs were measured by western blot. Cells were treated as above and subjected to western blot analysis. COX IV was used as a mitochondrial fraction loading control. β-actin and H3 were used as cytoplasmic fraction loading control and nuclear fraction loading control respectively. Data are expressed as mean ± S.E.M. Representative results of three experiments are shown (* $P < 0.05$ and ** $P < 0.01$).

further examined the change of MMP. As expected, flow cytometry analysis and immunoflurescence results showed that GO/G treatment induced mitochondrial depolarization in a time-dependent manner. Moreover, it's well known that accumulated PAR polymer via PARP-1 activation facilitates the nucleus translocation of AIF from the mitochondria by binding to AIF [16], therefore we detected the mitochondria, cytoplasm and nucleus AIF levels. Consistent with above findings, the data confirmed the translocation of AIF into the nucleus and induced nuclear condensation upon exposure of MCs to GO/G. Overactivation of PARP-1 plays a pivotal role in the initiation of parthanatos. The PAR polymer, product of PARP-1 activation, is regarded as a key effector of parthanatos [15]. In this study, we found that PARP-1 knockdown not only ameliorated GO/G-induced collapse of MMP and MCs death, but also diminished the accumulation of PAR polymer and nuclear AIF levels. These results indicated that GO/G-induced cell death and AIF translocation were mediated by PARP-1 activation, which is in accordance with the primary characteristics of parthanatos. Coupled with our previous published data [37], we speculated that multiple cell death pathways including caspase-dependent apoptosis and parthanatos were involved in oxidative stress-induced MCs death.

Basal levels of autophagy plays vital roles in the homeostatic process and exerts as a pro-survival mechanism in physiological conditions and pathological conditions, such as nutrient deprivation and microbial infection [49]. However, autophagy can also serve as a prodeath mechanism in certain circumstances [49,50]. Previous studies had shown that PARP-1 participated in modulation of oxidative stress-induced autophagy and such autophagy served a cytoprotective function in ROS-mediated necrosis [51]. Our current study first confirmed that parthanatos and autophagy co-existed in GO/G induced MCs damage. More importantly, our data demonstrated that PARP-1 knockdown inhibited the induction of autophagy as revealed by the decreased conversion of LC3-I to LC3-II and increased levels of p62. This observation supported the view that PARP-1 activation is involved in the decision making process for cell to undergo autophagy, which is consistent with previous reports in MEFs [51]. Considering the regulation of PARP-1 in these two process, we speculated that there might be a direct link between parthanatos and autophagy. PARP-1 activation induced by GO/G triggered a cell response with two components: cell death with characteristics of parthanatos and autophagy. Currently, the functional role of GO/G-induced autophagy in MCs remains unknown. Based on our flow cytometry results, inhibition of autophagy by 3-MA sensitized MCs to GO/G-induced cell death, suggesting autophagy as a cytoprotective factor against GO/G-induced cell death. In addition, the interplay between autopagy and parthanatos remains controversial. Huang et al.

[52]. reported that cell undergoing parthanatos was irresponsive to bafilomycin A1, and insensitive to enforced autophagy induction by mTORC1 inhibition. However, in our study, we found that autophagy inhibition by 3-MA aggravated GO/G-induced MMP decline, simultaneously upregulated PARP-1 expression and increased the PAR polymer synthesis, which facilitated AIF translocation to nucleus and aggravated subsequent nuclear damage. Thus, all these data led to the conclusion that autophagy performed a pro-survival role in MCs to antagonize GO/G-induced parthanatos. Autophagy may achieve the beneficial effect through the elimination of damaged mitochondria [53]. Inside the cell, mitochondria are the principal site of ROS generation and also the susceptible targets for ROS damage, thus oxidative stress is closely associated with mitochondrial dysfunction [54]. The accumulation of dysfunctional mitochondria, in turn, can lead to further amplification of oxidative stress and cause cell death. Thus autophagy of mitochondria, can promote cell survival by maintaining a healthy pool of mitochondria and cellular homeostasis.

PARP-1 appears to play a dual role during the response of cell to GO/G. On one hand, PARP-1 activation is the cause of parthanatos via inducing AIF nuclear translocation. On the other hand, PARP-1 activation is able to elicit a pro-survival autophagy. The explanation for this paradoxical phenomenon maybe is that GO/G at early time points generates mild levels of ROS and causes mild activation of PARP-1, not directly triggering cell death but allowing the cell to engage pro-survival autophagy and DNA repair. Once reaching a certain threshold of oxidative stress, PARP-1 can be overactivated, causing depletion of NAD+ and ATP, leading to cellular energy failure and parthanatos. Thus, the final fate of cells may be dependent on the balance between autophagy and parthanatos.

In conclusion, our present study demonstrated that GO/G treatment initiated PARP-1-dependent parthanatos via overactivation of PARP-1, excessive accumulation of PAR polymer, mitochondrial depolarization, and AIF nuclear translocation in MCs. Furthermore, GO/G stimulation induced autophagy which served as a protective factor against GO/G-induced parthanatos, and PARP-1 knockdown decreased GO/G-induced autophagy in MCs. These findings may provide us with better understanding of the relationship among oxidative stress, autophagy and parthanatos, and shed light on the new therapeutic interventions for ameliorating oxidative stress-related hearing disorders.

Acknowledgements

This work was supported by grants from National Natural Science Foundation of China (Nos. 81230021 and 81600804) and the Major State Basic Research Development Program of China (973 program) (No. 2011CB504504).

Conflict of interest

The authors declare no conflict of interest.

References

[1] T.S. Kim, J.W. Chung, Evaluation of age-related hearing loss, Korean J. Audiol. 17 (2013) 50–53.
[2] H.F. Schuknecht, M.R. Gacek, Cochlear pathology in presbycusis, Ann. Otol. Rhinol. Laryngol. 102 (1993) 1–16.
[3] E. Tavanai, G. Mohammadkhani, Role of antioxidants in prevention of age-related hearing loss: a review of literature, Eur. Arch. Otorhinolaryngol. 274 (2017) 1821–1834.
[4] R.S. Sohal, R. Weindruch, Oxidative stress, caloric restriction, and aging, Science 273 (1996) 59–63.
[5] M. Rigoulet, E.D. Yoboue, A. Devin, Mitochondrial ROS generation and its regulation: mechanisms involved in H(2)O(2) signaling, Antioxid. Redox Signal. 14 (2011) 459–468.
[6] H.F. Schuknecht, K. Watanuki, T. Takahashi, A.A. Belal Jr., R.S. Kimura, D.D. Jones, C.Y. Ota, Atrophy of the stria vascularis, a common cause for hearing loss, Laryngoscope 84 (1974) 1777–1821.
[7] P. Wangemann, Supporting sensory transduction: cochlear fluid homeostasis and the endocochlear potential, J. Physiol. 576 (2006) 11–21.
[8] K.K. Ohlemiller, Mechanisms and genes in human strial presbycusis from animal models, Brain Res. 1277 (2009) 70–83.
[9] W.L. Kraus, M.O. Hottiger, PARP-1 and gene regulation: progress and puzzles, Mol. Aspects Med. 34 (2013) 1109–1123.
[10] I. Lonskaya, V.N. Potaman, L.S. Shlyakhtenko, E.A. Oussatcheva, Y.L. Lyubchenko, V.A. Soldatenkov, Regulation of poly(ADP-ribose) polymerase-1 by DNA structure-specific binding, J. Biol. Chem. 280 (2005) 17076–17083.
[11] W.X. Zong, D. Ditsworth, D.E. Bauer, Z.Q. Wang, C.B. Thompson, Alkylating, DNA damage stimulates a regulated form of necrotic cell death, Genes Dev. 18 (2004) 1272–1282.
[12] H.C. Ha, S.H. Snyder, Poly(ADP-ribose) polymerase is a mediator of necrotic cell death by ATP depletion, Proc. Natl. Acad. Sci. USA 96 (1999) 13978–13982.
[13] L. Virag, C. Szabo, The therapeutic potential of poly(ADP-ribose) polymerase inhibitors, Pharmacol. Rev. 54 (2002) 375–429.
[14] A. Galia, A.E. Calogero, R. Condorelli, F. Fraggetta, A. La Corte, F. Ridolfo, P. Bosco, R. Castiglione, M. Salemi, PARP-1 protein expression in glioblastoma multiforme, Eur. J. Histochem. 56 (2012) e9.
[15] S.A. Andrabi, N.S. Kim, S.W. Yu, H. Wang, D.W. Koh, M. Sasaki, J.A. Klaus, T. Otsuka, Z. Zhang, R.C. Koehler, P.D. Hurn, G.G. Poirier, V.L. Dawson, T.M. Dawson, Poly(ADP-ribose) (PAR) polymer is a death signal, Proc. Natl. Acad. Sci. USA 103 (2006) 18308–18313.
[16] Y. Wang, V.L. Dawson, T.M. Dawson, Poly(ADP-ribose) signals to mitochondrial AIF: a key event in parthanatos, Exp. Neurol. 218 (2009) 193–202.
[17] K.K. David, S.A. Andrabi, T.M. Dawson, V.L. Dawson, Parthanatos, a messenger of death, Front. Biosci. 14 (2009) 1116–1128.
[18] S.A. Andrabi, T.M. Dawson, V.L. Dawson, Mitochondrial and nuclear cross talk in cell death: parthanatos, Ann. N. Y. Acad. Sci. 1147 (2008) 233–241.
[19] S.W. Yu, H. Wang, M.F. Poitras, C. Coombs, W.J. Bowers, H.J. Federoff, G.G. Poirier, T.M. Dawson, V.L. Dawson, Mediation of poly(ADP-ribose) polymerase-1-dependent cell death by apoptosis-inducing factor, Science 297 (2002) 259–263.
[20] G. Filomeni, D. De Zio, F. Cecconi, Oxidative stress and autophagy: the clash between damage and metabolic needs, Cell Death Differ. 22 (2015) 377–388.
[21] D. Glick, S. Barth, K.F. Macleod, Autophagy: cellular and molecular mechanisms, J. Pathol. 221 (2010) 3–12.
[22] B. Levine, G. Kroemer, Autophagy in aging, disease and death: the true identity of a cell death impostor, Cell Death Differ. 16 (2009) 1–2.
[23] G. Marino, M. Niso-Santano, E.H. Baehrecke, G. Kroemer, Self-consumption: the interplay of autophagy and apoptosis, Nat. Rev. Mol. Cell Biol. 15 (2014) 81–94.
[24] D.C. Rubinsztein, P. Codogno, B. Levine, Autophagy modulation as a potential therapeutic target for diverse diseases, Nat. Rev. Drug Discov. 11 (2012) 709–730.
[25] J.M. Rodriguez-Vargas, M.J. Ruiz-Magana, C. Ruiz-Ruiz, J. Majuelos-Melguizo, A. Peralta-Leal, M.I. Rodriguez, J.A. Munoz-Gamez, M.R. de Almodovar, E. Siles, A.L. Rivas, M. Jaattela, F.J. Oliver, ROS-induced DNA damage and PARP-1 are required for optimal induction of starvation-induced autophagy, Cell Res. 22 (2012) 1181–1198.
[26] J.A. Munoz-Gamez, J.M. Rodriguez-Vargas, R. Quiles-Perez, R. Aguilar-Quesada, D. Martin-Oliva, G. de Murcia, J. Menissier de Murcia, A. Almendros, M. Ruiz de Almodovar, F.J. Oliver, PARP-1 is involved in autophagy induced by DNA damage, Autophagy 5 (2009) 61–74.
[27] L. Virag, A. Robaszkiewicz, J.M. Rodriguez-Vargas, F.J. Oliver, Poly(ADP-ribose) signaling in cell death, Mol. Aspects Med. 34 (2013) 1153–1167.
[28] Z.T. Chen, W. Zhao, S. Qu, L. Li, X.D. Lu, F. Su, Z.G. Liang, S.Y. Guo, X.D. Zhu, PARP-1 promotes autophagy via the AMPK/mTOR pathway in CNE-2 human nasopharyngeal carcinoma cells following ionizing radiation, while inhibition of autophagy contributes to the radiation sensitization of CNE-2 cells, Mol. Med. Rep. 12 (2015) 1868–1876.
[29] J.M. Mates, F.M. Sanchez-Jimenez, Role of reactive oxygen species in apoptosis: implications for cancer therapy, Int. J. Biochem. Cell Biol. 32 (2000) 157–170.
[30] J. Nordberg, E.S. Arner, Reactive oxygen species, antioxidants, and the mammalian thioredoxin system, Free Radic. Biol. Med. 31 (2001) 1287–1312.
[31] H.J. Forman, M. Torres, Redox signaling in macrophages, Mol. Aspects Med. 22 (2001) 189–216.
[32] B. Chance, H. Sies, A. Boveris, Hydroperoxide metabolism in mammalian organs, Physiol. Rev. 59 (1979) 527–605.
[33] F. Antunes, E. Cadenas, Estimation of H2O2 gradients across biomembranes, FEBS Lett. 475 (2000) 121–126.
[34] X.Y. Zhao, J.L. Sun, Y.J. Hu, Y. Yang, W.J. Zhang, Y. Hu, J. Li, Y. Sun, Y. Zhong, W. Peng, H.L. Zhang, W.J. Kong, The effect of overexpression of PGC-1alpha on the mtDNA4834 common deletion in a rat cochlear marginal cell senescence model, Hear. Res. 296 (2013) 13–24.
[35] I. Melichar, A.H. Gitter, Primary culture of vital marginal cells from cochlear explants of the stria vascularis, Eur. Arch. Otorhinolaryngol. 248 (1991) 358–365.
[36] H.N. Kim, M.S. Chang, M.H. Chung, K. Park, Establishment of primary cell culture from stria vascularis explants, Morphological and functional characterization, Acta Otolaryngol. 116 (1996) 805–811.
[37] Y. Zhang, Y. Yang, Z. Xie, W. Zuo, H. Jiang, X. Zhao, Y. Sun, W. Kong, Decreased Poly(ADP-Ribose) Polymerase 1 Expression Attenuates Glucose Oxidase-Induced Damage in Rat Cochlear Marginal Strial Cells, Mol. Neurobiol. 53 (2016) 5971–5984.
[38] Y. Liu, X. Feng, Y. Zhang, H. Jiang, X. Cai, X. Yan, Z. Huang, F. Mo, W. Yang, C. Yang, S. Yang, X. Liu, Establishment and characterization of a novel osteosarcoma cell line: CHOS, J. Orthop. Res. 34 (2016) 2116–2125.
[39] L. Zheng, C. Wang, T. Luo, B. Lu, H. Ma, Z. Zhou, D. Zhu, G. Chi, P. Ge, Y. Luo, JNK Activation Contributes to Oxidative Stress-Induced Parthanatos in Glioma Cells via

Increase of Intracellular ROS Production, Mol. Neurobiol. 54 (2017) 3492–3505.
[40] Q. Zhang, D. Hou, Z. Luo, P. Chen, B. Lv, L. Wu, Y. Ma, Y. Chu, H. Liu, F. Liu, S. Yu, J. Zhang, D. Yang, J. Liu, The novel protective role of P27 in MLN4924-treated gastric cancer cells, Cell Death Dis. 6 (2015) e1867.
[41] L. Delavallee, L. Cabon, P. Galan-Malo, H.K. Lorenzo, S.A. Susin, AIF-mediated caspase-independent necroptosis: a new chance for targeted therapeutics, IUBMB Life 63 (2011) 221–232.
[42] Y. Lee, H.C. Kang, B.D. Lee, Y.I. Lee, Y.P. Kim, J.H. Shin, Poly (ADP-ribose) in the pathogenesis of Parkinson's disease, BMB Rep. 47 (2014) 424–432.
[43] G. Mohammad, M.M. Siddiquei, A.M. Abu El-Asrar, Poly (ADP-ribose) polymerase mediates diabetes-induced retinal neuropathy, Mediators Inflamm. 2013 (2013) 510451.
[44] Z. Yang, L. Li, L. Chen, W. Yuan, L. Dong, Y. Zhang, H. Wu, C. Wang, PARP-1 mediates LPS-induced HMGB1 release by macrophages through regulation of HMGB1 acetylation, J. Immunol. 193 (2014) 6114–6123.
[45] P. Lu, A. Kamboj, S.B. Gibson, C.M. Anderson, Poly(ADP-ribose) polymerase-1 causes mitochondrial damage and neuron death mediated by Bnip3, J. Neurosci. 34 (2014) 15975–15987.
[46] D. Ma, B. Lu, C. Feng, C. Wang, Y. Wang, T. Luo, J. Feng, H. Jia, G. Chi, Y. Luo, P. Ge, Deoxypodophyllotoxin triggers parthanatos in glioma cells via induction of excessive ROS, Cancer Lett. 371 (2016) 194–204.
[47] N. Zhao, Y. Mao, G. Han, Q. Ju, L. Zhou, F. Liu, Y. Xu, X. Zhao, YM155, a survivin suppressant, triggers PARP-dependent cell death (parthanatos) and inhibits esophageal squamous-cell carcinoma xenografts in mice, Oncotarget 6 (2015) 18445–18459.
[48] L.Y. Chiu, F.M. Ho, S.G. Shiah, Y. Chang, W.W. Lin, Oxidative stress initiates DNA damager MNNG-induced poly(ADP-ribose)polymerase-1-dependent parthanatos cell death, Biochem. Pharmacol. 81 (2011) 459–470.
[49] N. Mizushima, B. Levine, A.M. Cuervo, D.J. Klionsky, Autophagy fights disease through cellular self-digestion, Nature 451 (2008) 1069–1075.
[50] W.Q. Zuo, Y.J. Hu, Y. Yang, X.Y. Zhao, Y.Y. Zhang, W. Kong, W.J. Kong, Sensitivity of spiral ganglion neurons to damage caused by mobile phone electromagnetic radiation will increase in lipopolysaccharide-induced inflammation in vitro model, J. Neuroinflammation 12 (2015) 105.
[51] Q. Huang, Y.T. Wu, H.L. Tan, C.N. Ong, H.M. Shen, A novel function of poly(ADP-ribose) polymerase-1 in modulation of autophagy and necrosis under oxidative stress, Cell Death Differ. 16 (2009) 264–277.
[52] C.T. Huang, D.Y. Huang, C.J. Hu, D. Wu, W.W. Lin, Energy adaptive response during parthanatos is enhanced by PD98059 and involves mitochondrial function but not autophagy induction, Biochim. Biophys. Acta 2014 (1843) 531–543.
[53] J. Lee, S. Giordano, J. Zhang, Autophagy, mitochondria and oxidative stress: cross-talk and redox signalling, Biochem. J. 441 (2012) 523–540.
[54] M.P. Murphy, How mitochondria produce reactive oxygen species, Biochem. J. 417 (2009) 1–13.